Gy without bFGF (REF *10*). These data indicate that although ASMase-mediated microvascular endothelial apoptosis is the prevailing mechanism for induction of the GI syndrome at WBR doses <18 Gy, an alternative mechanism, perhaps involving direct damage to stem cells, is engaged by higher radiation doses.

Our studies provide evidence that radiation damage to GI stem cell clonogens, regarded as the critical lesion in the pathogenesis of the GI syndrome, is a consequence of extensive microvascular injury. The vulnerability of the microvascular endothelium to stress appears related to the abundance of ASMase in endothelium (20 times as much as in other cell types) (*22*) and to its preferential trafficking to the plasma membrane. ASMase exists in lysosomal and secretory isoforms (*23*), both produced by posttranscriptional processing of a single gene product. The secretory isoform targets the plasma membrane, may reside in caveolar microdomains (*24*), and is also found extracellularly at the cell surface (*23, 24*). Further, inflammatory cytokines, such as interleukin-1β and interferon-γ, increase ASMase secretion threefold (*22*), indicating that under stress, endothelial cells mobilize excess amounts of membrane-targeted ASMase.

The specific sensitivity of microvascular versus large vessel endothelium to stress may be associated with bFGF distribution within vascular basement membranes. Although bFGF is ubiquitously expressed in basement membranes of large and intermediate size blood vessels, microvascular basement membranes have minimal or absent bFGF deposits (*25*). Ultrastructural studies indicate that capillaries represent the most radiation-sensitive sections of the vascular system (*26*). Because basement membrane–bound bFGF protects endothelial cells against radiation-induced cell death in vitro (*27*), its lack of expression in microvascular basement membranes may render this section of the vascular system highly sensitive to ASMase-mediated apoptosis.

Finally, our studies suggest that small molecules, such as bFGF, may improve the therapeutic ratio during WBR for leukemia, and abdominal radiation therapy for gastrointestinal, genitourinary, and gynecological tumors. A potential for therapeutic gain would likely be limited to patients in whom tissue typing demonstrates tumors to be insensitive to bFGF. Further, we propose that a requirement for ASMase-mediated ceramide generation in induction of microvascular endothelial apoptosis, and its inhibition by bFGF, represent a generic model for evolution of and protection against normal tissue damage after environmental, chemical, or toxic stress.

References and Notes

1. C. S. Potten, *Int. J. Radiat. Biol.* **58**, 925 (1990).
2. C. S. Potten *et al.*, *Int. J. Exp. Pathol.* **78**, 219 (1997).
3. C. Booth, C. S. Potten, *J. Clin. Invest.* **105**, 1493 (2000).
4. C. W. Houchen *et al.*, *Am. J. Physiol.* **276**, G249 (1999).
5. P. Okunieff *et al.*, *Radiat. Res.* **150**, 204 (1998).
6. W. B. Khan *et al.*, *Radiat. Res.* **148**, 248 (1997).
7. P. Santana *et al.*, *Cell* **86**, 189 (1996).
8. L. A. Pena *et al.*, *Cancer Res.* **60**, 321 (2000).
9. P. Okunieff *et al.*, *Br. J. Cancer Suppl.* **27**, S105 (1996).
10. F. Paris , R. Kolesnick, unpublished data.
11. Late-stage and early-stage apoptosis were assessed by TUNEL (*7*) and by in situ labeling with annexin V [A. L. Bronckers *et al.*, *Histochem. Cell Biol.* **113**, 293 (2000)]. To identify endothelial cells, we immunostained tissue with a rat monoclonal antibody against CD31 as in (*16*), except that we used a biotinylated rabbit antibody directed against a rat secondary antibody (1:100 dilution) and omitted the counterstaining. For annexin V staining, we injected mice iv with 0.5 mg of annexin V–FITC (Sigma, St Louis, MO) and killed mice 30 min later by hypercapnia asphyxiation. Tissue sections were counterstained with propidium iodide and scored by fluorescence microscopy.
12. C. S. Potten, H. K. Grant, *Br. J. Cancer* **78**, 993 (1998).
13. A. J. Merritt *et al.*, *Oncogene* **14**, 2759 (1997).
14. A. J. Merritt, L. S. Jones, C. S. Potten, in *Techniques in Apoptosis* T. G. Cotter, S. J. Martin, Eds. (Portland Press, London, 1996), pp. 269–299.
15. Supplementary material is available on *Science* Online at www.sciencemag.org/cgi/content/full/293/5528/293/DC1
16. A. Haimovitz-Friedman *et al.*, *J. Exp. Med.* **186**, 1831 (1997).
17. N. H. Terry, E. L. Travis, *Int. J. Radiat. Oncol. Biol. Phys.* **17**, 569 (1989).
18. Mouse *FGFR* cDNA sequences were incorporated into pBluescript SK^{50} plasmids, and included *FGFR 1b, 1c, 2b, 2c, 3b, 3c*, and *FGFR-4* [D.M.Ornitz *et al.*, *J. Biol. Chem.* **271**, 15292 (1996)]. *FGFR-1* and *FGFR-3* probes were generated by polymerase chain reaction using specific primers to produce T3 promoter-tailed DNA fragments. These were subsequently used as templates to transcribe the sense and antisense riboprobe with T3 polymerase. *FGFR-2* and *FGFR-4* probes were transcribed from the pBluescript SK^{50} plasmids. Recombinant plasmid (1 μg) was linearized by Bgl II and Nhe I, or Nco I and Not I, respectively, to generate sense and antisense transcripts. Riboprobes were generated with T7 and T3 polymerases for 2 hours at 37°C in 1× transcription buffer (Boehringer Mannheim, Indianapolis) containing 20 U of RNase inhibitor; 1 mmol/liter each of ATP, GTP, and CTP; 6.5 mmol/liter of UTP; and 3.5 mmol/liter of digoxigenin-UTP. In situ hybridization was carried out by using deparaffinized tissue sections rinsed in water and phosphate-buffered saline for 10 min. Slides were digested in prewarmed citrate buffer for 5 min in a microwave. Prehybridization was performed for 30 min at 45°C in 50% deionized formamide and 2× SSC. For hybridization, 10 pmol/liter of digoxigenin-labeled riboprobe was added to 50 μl hybridization buffer [50% deionized formamide (v/v), 10% dextran sulfate, 2× SSC, 1% SDS, and 0.25 mg/ml of herring sperm DNA]. After overnight incubation at 45°C, slides were washed twice for 20 min in prewarmed 2× SSC at 42°C, followed by two washes in prewarmed 1× SSC at 42°C for 20 min. Slides were then incubated in normal sheep serum diluted in buffer 1 (2 M Tris HCl, 5 M NaCl, pH 7.5). In some experiments, slides were incubated in the same buffer with antibody against digoxigenin-AP (Boehringer Mannheim, Indianapolis, IN) at a dilution of 1:500 for 1 hour at room temperature. Visualization of hybridized transcripts was accomplished by nitroblue tetrazolium 5-bromo-4-chloro-3-indolylphosphate. Slides were counterstained with methyl green and mounted. In other experiments, hybridization was at 42°C and slides were incubated with antibody against digoxigenin-rhodamine (Boehringer Mannheim) at a dilution of 1:200 for 1 hour at 37°C, in the dark. Slides were counterstained in 4,6-diamino-2-phenylindole (DAPI), mounted, and examined by using a fluorescent microscope (Olympus VX40) with blue and red filters.
19. P. Capodieci *et al.*, *Diagn. Mol. Pathol.* **7**, 69 (1998).
20. C. Magi-Galluzzi *et al.*, *Lab. Invest.* **76**, 37 (1997).
21. H. Fahimi, E. Baumgart, *J. Histochem. Cytochem.* **47**, 1219 (1999).
22. S. Marathe *et al.*, *J. Biol. Chem.* **273**, 4081 (1998).
23. S. L. Schissel *et al.*, *J. Biol. Chem.* **273**, 18250 (1998).
24. R. T. Dobrowsky, V. R. Gazula, *Methods Enzymol.* **311**, 184 (2000).
25. C. Cordon-Cardo *et al.*, *Lab. Invest.* **63**, 832 (1990).
26. H. S. Reinhold, L. F. Fajardo, J. W. Hopewell, *Adv. Radiat. Biol.* **14**, 177 (1990).
27. Z. Fuks *et al.*, *Eur. J. Cancer* **28A**, 725 (1992).
28. E. L. Kaplan, P. Meyer, *J. Am. Stat. Assoc.* **53**, 447 (1958).
29. N. Mantel, *Cancer Chemother. Rep.* **50**, 163 (1966).
30. C. Cordon-Cardo, P. Capodieci, unpublished data.

31. We thank S. Jio for outstanding technical support and M. Goldfarb for the *FGFR* cDNAs. These studies were supported by grants CA85704 (R.K.) and CA52462 (Z.F.), and a Fellowship from the Association pour la Recherche sur le Cancer (F.P.).

26 February 2001; accepted 25 May 2001

Molecular Evolution of Protein Atomic Composition

Peggy Baudouin-Cornu,[1] Yolande Surdin-Kerjan,[1] Philippe Marlière,[2] Dominique Thomas[1]*

Living organisms encounter various growth conditions in their habitats, raising the question of whether ecological fluctuations could alter biological macromolecules. The advent of complete genome sequences and the characterization of whole metabolic pathways allowed us to search for such ecological imprints. Significant correlations between atomic composition and metabolic function were found in sulfur- and carbon-assimilatory enzymes, which appear depleted in sulfur and carbon, respectively, in both the bacterium *Escherichia coli* and the eukaryote *Saccharomyces cerevisiae*. In addition to genetic instructions, genomic data thus also provide paleontological records of environmental nutrient availability and of metabolic costs.

A widely accepted principle is that protein evolution is mainly determined by constraints on activity, specificity, folding, and stability (*1–4*). But other constraints may come into play, in particular nutritional constraints, which have thus far received little scrutiny. Indeed, the elements used in the construction of proteins are not only funneled through metabolic pathways but are also subject to geochemical cycles at the surface of Earth.

Thus, we previously proposed that metabolic flows and geochemical budgets might be constraints that were imprinted on protein evolution (*5*).

To assess the hypothesis that nutritional constraints might have influenced the evolution of protein structure, we computed the atomic composition of enzymes involved in elemental assimilation processes in the two model microorganisms *E. coli* and *S. cerevisiae*. For both species, almost complete sets of biochemically characterized enzymes together with their cognate sequences are available, allowing us to analyze species representing the prokaryotic and eukaryotic kingdoms. We began by compiling complete protein sequence data sets from the nonredundant *Saccharomyces* Genome Database (SGD; http://genome-www.stanford.edu/Saccharomyces, 6305 protein sequences) and the Colibri *E. coli* database (http://genolist.pasteur.fr/Colibri, 4116 protein sequences).

We first investigated sulfur usage in sequences of proteins involved in the assimilation of sulfur in *S. cerevisiae* and *E. coli*. In both organisms, reductive assimilation of sulfate is achieved through roughly equivalent sets of biochemical reactions (*6, 7*). However, some differences were apparent. For instance, the reactions leading to the incorporation of reduced sulfur into a carbon chain differ between the two organisms; homocysteine is an intermediate of cysteine synthesis in yeast but not in *E. coli* (*8*). In addition, in some particular steps such as sulfate activation and sulfite reduction, the reactions proceed with different mechanisms and therefore the structures of the cognate catalysts are highly divergent (*9, 10*). The protein sets used for the statistical analyses include, for both organisms, the inorganic sulfur transporters, the enzymes required for the de novo synthesis of methionine and cysteine from sulfate, and the transcriptional activators specifically required for the expression of the corresponding genes (*6, 7, 11*). These sets comprise 20 and 23 proteins for *S. cerevisiae* and *E. coli*, respectively.

To compare elemental composition in proteins, we first determined the quantile distribution of atoms in proteins. This approach relies on that developed by Karlin and collaborators for the analysis of amino acid distribution in large protein data sets (*12, 13*). In this study, the quantity $Q(x)$ (quantile point) of a given element for a given set of proteins indicates the fraction of proteins in which the averaged number of that atom per residue side chain is at most x (*14*).

For both *S. cerevisiae* and *E. coli*, we compared the quantile distribution of the sulfur metabolism protein set to the quantile distribution of the total protein set (Fig. 1). In both cases, despite differences in sulfur metabolism between the two organisms, the proteins involved in sulfur amino acid biosynthesis contain fewer sulfur atoms than do the total protein sets. In both the sulfur-assimilatory protein sets and the total protein sets, the distribution of sulfur content follows a bell-shaped distribution that is approximately Gaussian (Fig. 1). We thus assessed statistical significance with Student's t tests. Two-tailed P values (0.0038 for *S. cerevisiae*, 0.0089 for *E. coli*) confirm that, in both cases, the differences observed between the distributions are significant.

Biases of chemical composition of proteins could result from constraints that are not related to element usage or metabolism, such as structural and functional constraints or molecular phylogeny (*15*). For instance, not all amino acids show the same propensity to form secondary structures such as α helices, β sheets, or turns, and binding of substrates is often mediated by hydrophobic or charged amino acids. Also, amino acid usage of bulk proteins is known to correlate with DNA base composition (*16, 17*). These alternative hypotheses can be dismissed in the biases we observed in the sulfur-assimilatory pathways: The involved proteins belong to diverse catalytic classes, encompass a wide variety of tertiary structures, and process widely diverging substrates (*7*). In addition, the base composition of the corresponding genes does not statistically deviate from that of the organism (*18*), arguing against the possibility that the observed biases result from coding constraints. Moreover, *S. cerevisiae* and *E. coli* genomes have different G+C contents (40% and 52% GC in the coding sequences, respectively), and despite this, sulfur depletion was observed in the sulfur-assimilatory pathway of both organisms. It therefore seems reasonable to postulate that a bias against sulfur-containing amino acids occurred in response to nutritional constraints such as environmental sulfur scarcity.

To further test this hypothesis, we next examined proteins involved in sulfur metabolism in mammals. Mammals are unable to assimilate inorganic sulfur compounds, and therefore all their protein sulfur atoms derive from methionine and cysteine (*19*). Thus, mammals are not specifically deprived of sulfur without also lacking other essential nutrients, and sulfur atom avoidance would be expected to be less marked in mammalian sulfur-metabolizing enzymes. Mammals express only a few enzymes that are the functional equivalents of microbial sulfur-assimilatory enzymes (*19*). Sequence counts reveal that most of the mammalian enzymes indeed contain three to five times as many sulfur atoms as do their microbial counterparts (*18*). Sequence alignment of the two enzymes catalyzing the conversion of homocysteine into cysteine illuminates this effect. Mammalian cystathionine-β-synthase (CBS) and cystathionine-γ-lyase share more than 40% identical residues with their yeast homologs. However, the two yeast enzymes contain a total of 8 sulfur atoms, whereas 50 and 42 sulfur atoms are used to construct the rat and human enzymes, respectively (Fig. 2) (*20*). Despite these atomic differences, the human CBS enzyme can substitute in vivo for the *S. cerevisiae* CBS protein (*21*). Thus, in mammals, where no sulfur-specific nutritional constraint occurs, no sulfur depletion is observed in sulfur-metabolizing enzymes.

Sulfur is unique among the elemental constituents of proteins because it is used in only two amino acids: methionine and cys-

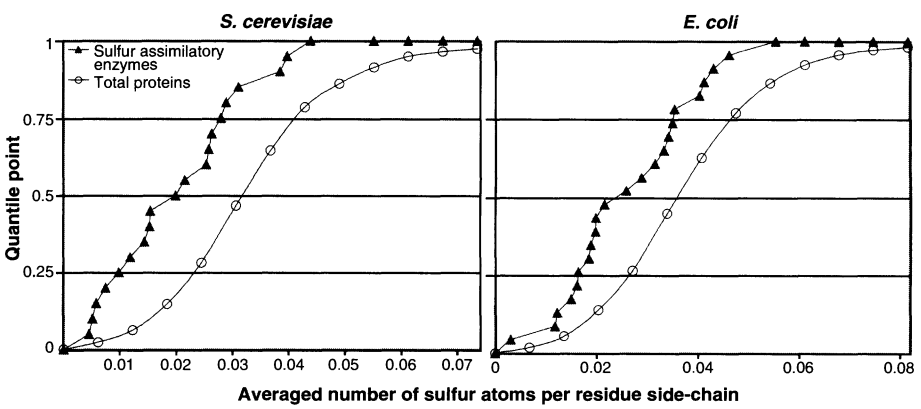

Fig. 1. Quantile representations of sulfur usage in *S. cerevisiae* and *E. coli*. For both species, the averaged number of sulfur atoms found in residue side chains for each protein was calculated, and the totality of all these frequencies was described by a histogram. The quantile distributions are the cumulative representation of these histograms. For each total protein set, the quantiles were calculated so as to display the distribution by a 13-dot graph. For the sulfur-assimilatory protein sets, the quantiles were indicated for each new value of the distribution.

[1]Centre de Génétique Moléculaire, Centre National de la Recherche Scientifique, 91 198 Gif-sur-Yvette Cedex, France. [2]Evologic SA, 4 rue Pierre Fontaine, 91000 Evry, France.

*To whom correspondence should be addressed. E-mail: thomas@cgm.cnrs-gif.fr

teine. To determine whether metabolic imprinting in atomic composition of proteins is a more general mechanism, we analyzed carbon usage in carbon-assimilatory proteins of both *S. cerevisiae* and *E. coli* (*22–24*). For each organism, we computed the averaged number of carbon atoms present within the side chains of residues of each protein, calculated quantile distributions of carbon, and made comparisons between the set of proteins involved in carbon assimilation and the total protein set. In both cases, carbon-assimilating proteins show a depleted amount of carbon atoms in their side chains relative to the side chains of the total protein sets (Fig. 3). The distribution of carbon atoms, like that of sulfur atoms, was approximately Gaussian, and Student's *t* tests gave two-tailed *P* values (0.0031 for *S. cerevisiae*, 0.0068 for *E. coli*), indicating significant differences between the distributions. By comparison, quantile carbon representations (Fig. 3) and statistical tests ($P = 0.364$ and 0.438, respectively) demonstrate that no carbon usage deviation occurs in the sulfur-assimilatory protein sets.

Finally, we compared the averaged number of nitrogen atoms present within the nitrogen-assimilatory *S. cerevisiae* proteins to that in the total *S. cerevisiae* protein set. The yeast nitrogen-assimilatory protein set consists of the proteins involved in the conversion of ammonia, urea, allantoate, and proline (*25, 26*). (No similar analysis was done for *E. coli* because all the enzymes involved in ammonia production from a number of amino acids have not been unambiguously determined.) As was the case for sulfur- and carbon-assimilating proteins, quantile representation shows that yeast nitrogen-assimilating proteins contain a decreased number of nitrogen atoms in their residue side chains, whereas no significant deviation in nitrogen usage was observed for the set comprising the yeast sulfur-assimilatory proteins, used as a control (Fig. 4). Again, the two-tailed *P* value (0.0331) in a Student's *t* test suggests that the observed difference does not occur by chance. However, both the quantile and Student's *t* test show that nitrogen bias, although significant, is less pronounced than the biases observed for the sulfur and carbon atoms in their cognate assimilatory enzymes.

Taken together, our results conclusively demonstrate the systematic occurrence of atomic biases in assimilatory proteins of two highly divergent microorganisms. This suggests that the elemental composition of biological polymers has been more generally subjected to ecological constraints than was previously thought, and that metabolic costs are among the variables optimized by natural selection. A simple explanation for the biases we report here is that the chemical structure of proteins performing the assimilation of a given element should evolve so as to respond to a sudden and transitory shortage by incorporating the smallest amount of that element. Thus, the impoverishment of sulfur- and carbon-assimilatory proteins in their respective elements can be interpreted as an imprint of variations in the nutritional availability of these elements during the natural history of *S. cerevisiae* and *E. coli*; by contrast, the enrichment of mammalian cystathionine-converting enzymes in sulfur can be interpreted as an imprint of a steady abundance of sulfur amino acids in the diet. It is likely that oligotrophic organisms would adapt to the permanent scarcity of an element by the diminution of the content of that element in all proteins, and not only in their assimilatory proteins for that element. Given that the proliferation of most organisms in their natural habitats is limited by a nutritional resource and that organisms have adapted to starvation over many generations, we anticipate that it will be possible to retrieve geochemical, ecological, and metabolic data from genome sequences using straightforward statistical methods.

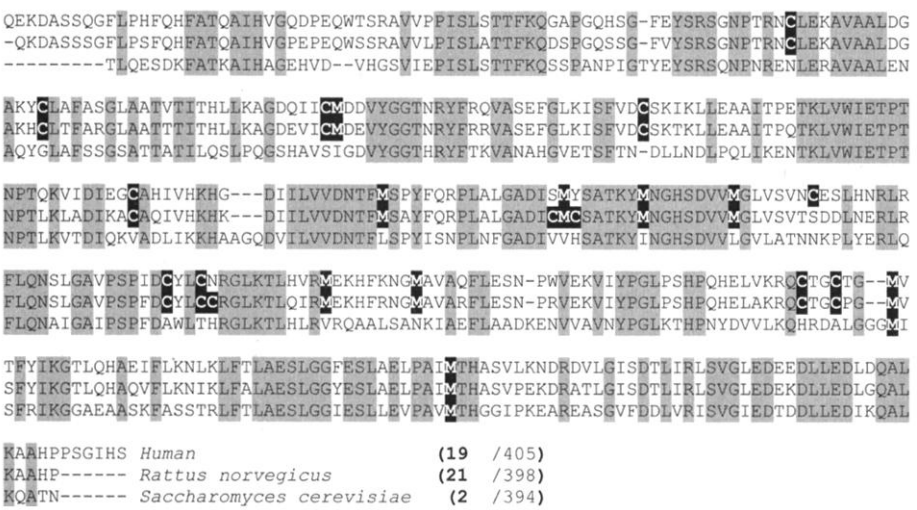

Fig. 2. Sulfur usage in cysteine biosynthetic enzymes. The human, rat, and yeast cystathionine-γ-lyase were aligned using the Clustal V program. Identical residues are indicated in gray boxes; sulfur-containing residues are in black boxes. Number of sulfur atoms relative to the length of protein is indicated. Single-letter abbreviations for amino acid residues: A, Ala; C, Cys; D, Asp; E, Glu; F, Phe; G, Gly; H, His; I, Ile; K, Lys; L, Leu; M, Met; N, Asn; P, Pro; Q, Gln; R, Arg; S, Ser; T, Thr; V, Val; W, Trp; and Y, Tyr.

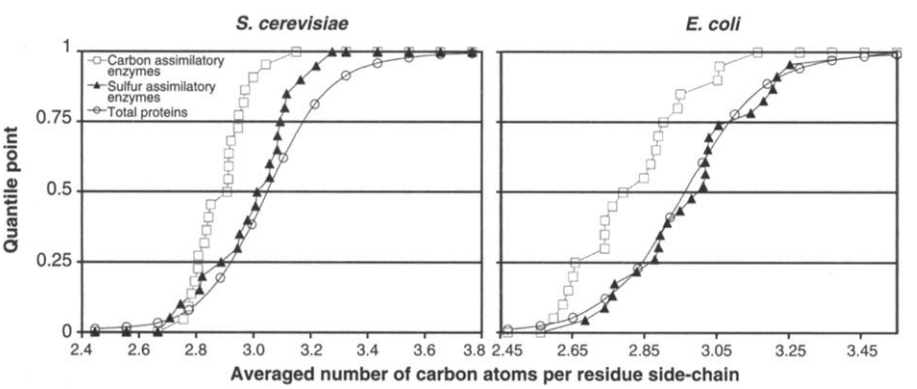

Fig. 3. Quantile representations of carbon usage in *S. cerevisiae* and *E. coli*. The quantiles were calculated and are displayed as in Fig. 1.

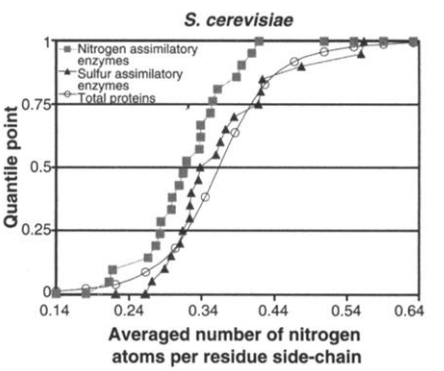

Fig. 4. Quantile representations of nitrogen usage in *S. cerevisiae*. The quantiles were calculated and are displayed as in Fig. 1.

References and Notes

1. M. Kimura, *The Neutral Theory of Molecular Evolution* (Cambridge Univ. Press, Cambridge, 1983).
2. M. Nei, *Molecular Evolutionary Genetics* (Columbia Univ. Press, New York, 1987).
3. W.-H. Li, *Molecular Evolution* (Sinauer, Sunderland, MA, 1997).
4. N. J. Tourasse, W.-H. Li, *Mol. Biol. Evol.* **17**, 656 (2000).
5. D. Mazel, P. Marlière, *Nature* **341**, 245 (1989).
6. N. M. Kredich, in Escherichia coli *and* Salmonella typhimurium, F. C. Neidhardt, Ed. (American Society for Microbiology, Washington, DC, 1996), pp. 419–429.
7. D. Thomas, Y. Surdin-Kerjan, *Microbiol. Mol. Biol. Rev.* **61**, 503 (1997).
8. H. Cherest, D. Thomas, Y. Surdin-Kerjan, *J. Bacteriol.* **175**, 5366 (1993).
9. T. S. Leyh, Y. Suo, *J. Biol. Chem.* **267**, 542 (1992).
10. T. S. Leyh, *Crit. Rev. Biochem. Mol. Biol.* **28**, 515 (1993).
11. For *S. cerevisiae*, the sulfur-assimilatory enzymes used for the statistical analyses were the *MET1, 2, 3, 4, 5, 6, 7, 8, 10, 13, 14, 16, 25, 28, 31, 32, STR1, STR4, SUL1*, and *SUL2* gene products. For *E. coli*, the enzymes used were the *CysA, B, C, D, E, G, H, I, J, K, M, N, P, U, W, Z, MetA, B, C, E, H, R*, and *Sbp* gene products.
12. S. Karlin, V. Brendel, *Science* **257**, 39 (1992).
13. S. Karlin, B. E. Blaisdell, P. Bucher, *Protein Eng.* **5**, 729 (1992).
14. For all the calculations reported here, the methionine initiating residues were removed from all the protein sequences.
15. T. E. Creighton, *Proteins: Structures and Molecular Properties* (Freeman, New York, 1983).
16. N. Suekoa, *Cold Spring Harbor Symp. Quant. Biol.* **26**, 35 (1961).
17. G. A. C. Singer, D. A. Hickey, *Mol. Biol. Evol.* **17**, 1581 (2000).
18. P. Baudouin-Cornu, Y. Surdin-Kerjan, P. Marlière, D. Thomas, data not shown.
19. O. W. Griffith, *Methods Enzymol.* **143**, 366 (1987).
20. Supplementary material is available on *Science* Online at www.sciencemag.org/cgi/content/full/293/5528/297/DC1.
21. W. D. Kruger, D. R. Cox, *Proc. Natl. Acad. Sci. U.S.A.* **91**, 6614 (1994).
22. D. G. Fraenkel, in Escherichia coli *and* Salmonella typhimurium, F. C. Neidhardt, Ed. (American Society for Microbiology, Washington, DC, 1996), pp. 189–198.
23. M. Johnston, M. Carlson, in *The Molecular and Cellular Biology of the Yeast* Saccharomyces, E. W. Jones, J. R. Pringle, J. R. Broach, Eds. (Cold Spring Harbor Laboratory Press, Cold Spring Harbor, NY, 1992), pp. 193–281.
24. For *S. cerevisiae*, the carbon-assimilatory enzymes used for the statistical analyses were the *ENO1, ENO2, FBA1, FBP1, GLK1, GMP1, HXK1, HXK2, PDC1, PDC5, PDC6, PFK1, PFK2, PGI1, PGK1, PYC1, PYK1, TDH1, TDH2, TDH3, TPI1*, and *ZWF1* gene products. For *E. coli*, the enzymes used were the *Eno, FbaA, GapA, Glk, Gnd, GpmA, PfkA, PfkB, Pgi, Pgk, Pgm, PykA, RpE, RpiA, RpiB, TalB, TktA, TktB, TpiA*, and *Zwf* gene products.
25. B. Magasanik, in *The Molecular and Cellular Biology of the Yeast* Saccharomyces, E. W. Jones, J. R. Pringle, J. R. Broach, Eds. (Cold Spring Harbor Laboratory Press, Cold Spring Harbor, NY, 1992), pp. 283–317.
26. The *S. cerevisiae* nitrogen-assimilatory enzymes used for the statistical analyses were the *DAL1, 2, 3, 4, 5, 7, 81, DUR3, DUR12, GDH1, GDH2, PUT1, 2, 3, 4, UGA1, 3, 4*, and *5* gene products.

27. Supported by a thesis fellowship from the Ministère de la Défense (P.B.-C.).

26 March 2001; accepted 1 June 2001

Impairment of Mycobacterial But Not Viral Immunity by a Germline Human *STAT1* Mutation

Stéphanie Dupuis,[1,2] Catherine Dargemont,[3] Claire Fieschi,[1] Nicolas Thomassin,[4] Sergio Rosenzweig,[5] Jeff Harris,[6] Steven M. Holland,[5] Robert D. Schreiber,[7] Jean-Laurent Casanova[1,8]*

Interferons (IFN) α/β and γ induce the formation of two transcriptional activators: gamma-activating factor (GAF) and interferon-stimulated gamma factor 3 (ISGF3). We report a natural heterozygous germline *STAT1* mutation associated with susceptibility to mycobacterial but not viral disease. This mutation causes a loss of GAF and ISGF3 activation but is dominant for one cellular phenotype and recessive for the other. It impairs the nuclear accumulation of GAF but not of ISGF3 in heterozygous cells stimulated by IFNs. Thus, the antimycobacterial, but not the antiviral, effects of human IFNs are principally mediated by GAF.

Mendelian susceptibility to mycobacterial disease is a rare syndrome (MIM 209950), leading to severe clinical infections with weakly virulent mycobacterial species, such as Bacillus Calmette-Guérin (BCG) vaccines (*1*) or environmental nontuberculous mycobacteria (*2*) and more virulent *Mycobacterium tuberculosis* (*3*). Other types of microorganisms rarely cause severe clinical disease, except for *Salmonella*, which infects less than half of the patients. Null recessive mutations have been identified in *IL12B* (*4*), encoding the p40 subunit of interleukin-12 (IL-12), in *IL12RB1* (*5*, *6*), encoding the β1 chain of the IL-12 receptor, in *IFNGR1* (*7*, *8*), and in *IFNGR2* (*9*), encoding the two chains of the IFN-γ receptor (IFN-γR). Recessive and dominant mutations, associated with partial IFN-γR, deficiency, have been found in *IFNGR1* (*3*, *10*) and *IFNGR2* (*11*). These studies established that human IL-12–dependent IFN-γ–mediated immunity is essential to control mycobacteria and provided means of molecular diagnosis and rational treatment based on pathophysiology. However, no clear genetic etiology has been identified for a number of patients.

We investigated two unrelated patients with unexplained mycobacterial disease. Proband 1 (P1) is a 33-year-old French woman who developed disseminated BCG infection in childhood (*12*). She had experienced many common viral infections, the clinical course of which was normal. Mutations in *IL12B* and *IL12RB1* had been excluded (*13*). We characterized cellular responses to IFN-γ by electrophoretic mobility shift assay (EMSA) using Epstein-Barr virus (EBV)–transformed B (EBV-B) cells. The level of nuclear-protein binding to gamma interferon–activating sequences (GAS) in P1 cells stimulated with IFN-γ (Fig. 1A) was 25 ± 3% of that in identically treated control cells (*14*). The GAS-binding protein, designated gamma-activating factor (GAF), consisted of STAT-1/STAT-1 homodimers (*13*). This profile was similar to that observed in partial IFN-γR1 and IFN-γR2 deficiency, but mutations in *IFNGR1* and *IFNGR2* were excluded (*13*). Moreover, only 25 ± 2% of the GAF detected in control cells was detected in P1 cells stimulated with IFN-α (*13*). Thus, the binding of nuclear STAT-1 homodimers to GAS was affected equally by IFN-γ and IFN-α in P1 cells.

We then analyzed the subcellular distribution of STAT-1 in simian virus 40 (SV40)–transformed fibroblasts (SV40 fibroblasts) by immunofluorescence (*15*). A smaller proportion of P1 STAT-1 accumulated in the nucleus upon IFN-γ stimulation than in control cells (Fig. 1B). This suggested that the smaller number of GAS-binding STAT-1 dimers

[1]Laboratoire de Génétique Humaine des Maladies Infectieuses, Université de Paris René Descartes–INSERM UMR550, Faculté de Médecine Necker-Enfants Malades, 75015 Paris, France. [2]INSERM U429, Hôpital Necker-Enfants Malades, 75015 Paris, France. [3]Institut Jacques Monod, CNRS–Université Paris VI–Université Paris VII–CNRS UMR7592, 75005 Paris, France. [4]Departement de Pédiatrie, Centre Hospitalier Général, 58000 Nevers, France. [5]Laboratory of Host Defenses, National Institute of Allergy and Infectious Diseases, Bethesda, MD 20892–1886, USA. [6]Department of Pediatrics, University of California at San Francisco, San Francisco, CA 94117, USA. [7]Department of Pathology, Washington University, St. Louis, MO 63110, USA. [8]Unité d'Hématologie-Immunologie Pédiatrique, Hôpital Necker-Enfants Malades, 75015 Paris, France.

*To whom correspondence should be addressed. E-mail: casanova@necker.fr